6-1-2021

Sound Speed Gradients in Mud

Charles W. Holland
Portland State University, hollan7@pdx.edu

Citation Details

Holland, C. W. (2021). Sound speed gradients in mud. *JASA Express Letters*, *1*(6), 066001. https://doi.org/10.1121/10.0005153

JASA EXPRESS LETTERS

Sound speed gradients in mud

Cite as: JASA Express Lett. **1**, 066001 (2021); https://doi.org/10.1121/10.0005153
Submitted: 16 April 2021 . Accepted: 13 May 2021 . Published Online: 07 June 2021

Charles W. Holland

JASA EXPRESS LETTERS ARTICLE asa.scitation.org/journal/jel

Sound speed gradients in mud

Charles W. Holland
Portland State University, Portland, Oregon 97201, USA
charles.holland@pdx.edu

Abstract: Various methods have been used to estimate sound speed profiles in mud at the New England Mud Patch. Some of these methods show large sound speed gradients of order $10\,s^{-1}$. New measurements of the seabed reflection coefficient exhibit an angle of intromission over three octaves in frequency; these data constrain the range of possible sound speed gradient values. The data indicate that sound speed gradients must be quite weak, i.e., much smaller than $|10\,s^{-1}|$. This conclusion is supported by core data which indicate nearly constant porosity in most of the mud layer.

[Editor: David R. Barclay] https://doi.org/10.1121/10.0005153

Received: 16 April 2021 **Accepted:** 13 May 2021 **Published Online:** 7 June 2021

1. Introduction

The acoustic properties of muddy sediments are poorly understood. For example, there are relatively few shallow-water measurements of the depth dependence of sound speed in mud layers. The goal of the multi-national Seabed Characterization Experiment (SBCEX17) was to improve understanding of muddy sediment acoustic properties. A significant aspect of the experiment was the large number and variety of experimental and inference methods applied to a limited region of the New England Mud Patch (NEMP), see Ref. 1. Experimental methods included inference from long-range acoustic propagation as well as more direct measurements based on *in situ* probes and cores.

One of the unresolved questions is the depth dependence of the mud in the upper few meters. This has been a deceptively difficult measurement to tie down. Some SBCEX17 results, including long-range propagation[2–4] and a method using inserted probes[5] indicate large mud sound speed gradients, of order $10\,s^{-1}$. These large gradients are surprising given that they were an order of magnitude higher than reasonably well-established values in deep-water muds.[6] Other NEMP measurements indicated that much of the mud layer had a small or negligible sound speed gradient, e.g., Refs. 7–9, at virtually the same geographic location. In sum, there is currently a wide range of estimated mud sound speed profiles that spans rapidly increasing sound speed with depth to nearly iso-speed to decreasing sound speeds (Fig. 8 AC-1 in Ref. 10) with depth.

This large disparity in mud sound speed profiles from different observations motivated the present work. The objective is to determine more definitively the NEMP near-surface sound speed gradients. The approach is to use data with a higher sediment sound speed information content than was previously available, in particular, direct-path seabed reflection coefficient observations.

The reflection data, windowed to probe the upper $\sim$2 m of sediment, show a clear angle of intromission across several octaves of frequency. The frequency-dependence of the angle of intromission contains high information content on mud sound speed depth dependence, e.g., Refs. 11 and 12. In Ref. 11, the frequency dependence was used to infer the depth dependence of the sound speed and density via Bayesian inversion. Instead, here, the data provide a useful observation by which various mud sound speed profiles can be assessed. This assessment is presented in Sec. 2 for various published sound speed profiles. Additional evidence for the limits of plausible mud sound speed gradients, both in the upper 2 m of sediment and deeper into the sediment column, is presented in Sec. 3 and conclusions are given in the final section.

2. Measurements

Direct path seabed reflection coefficient measurements were conducted at several locations at the NEMP; two are discussed here, Fig. 1. These measurements employed a fixed, bottom moored receiver and a towed broadband source towed in a radial from the receiver. Details on experiment design and data processing can be found in Ref. 13.

One of the advantages of directly measuring the seabed reflection coefficient is that the data can be time (depth) windowed to a specific layer or interface. Unless the surficial sediment sound speed, c_s, is precisely the same as the interstitial seawater, c_w, the reflection coefficient from the water-sediment interface will show either a critical angle (if $c_s > c_w$) or an angle of intromission (if $c_s < c_w$). Of the two possibilities, measuring the critical angle is far easier than measuring the angle of intromission. At the angle of intromission, the reflection coefficient drops to near zero. Thus, the challenge of its measurement is the challenge of measuring the absence of reflection. In addition to requiring a large signal-to-noise ratio, the experiment and data processing require the removal of all other contaminating paths. The challenge of making these

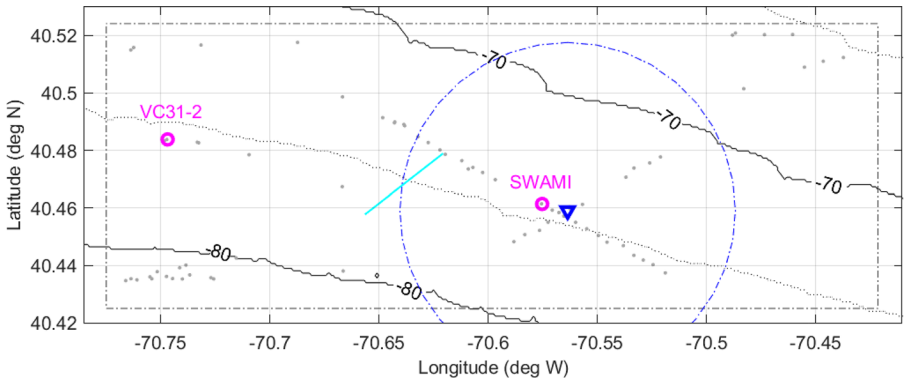

Fig. 1. Map of experiment area with bathymetry (m), cores (dots), seabed reflection coefficient measurements (open circles). The ARL-UT receive array location (blue triangle) and propagation track radius (blue dashed-dotted line) indicates the region probed by one of the propagation experiments (Ref. 2). Another propagation experiment track (Ref. 3) is also shown (cyan line).

measurements can be conveyed in part by noting that despite the considerable value of the angle of intromission for probing *in situ* fragile muddy sediments, measurements are quite scarce. To the author's knowledge, no prior angle of intromission measurements exist on the continental shelf of North or South America.

Here, we present and discuss reflection coefficient data collected in the central region of the experiment area where the mud layer is ∼10 m thick (SWAMI site, see Fig. 1). The reflection time series were processed to obtain the reflection coefficient, R, from the upper 1.7 m of mud. The data are presented as bottom loss ($-20\ \log_{10}|R|$), Fig. 2. The notable feature is the bottom loss peak, ∼8°, which is the angle of intromission. These data were shown at a single frequency in Ref. 13, along with inferences made assuming depth-independent geoacoustic properties. Here, we exploit the frequency-dependence of the angle of intromission, which contains information on the sound speed depth dependence.

If sediment sound speed is not constant with depth, the angle of intromission will be a function of frequency. This relationship is discussed in some detail, e.g., in Refs. 11 and 12. Nevertheless, in order to develop some intuition, it can be noted that if the mud sound speed increases with sediment depth, lower frequencies will be most sensitive to the deeper and higher sound speeds (which result in a lower angle of intromission) and higher frequencies will be sensitive to the near sediment-interface values with lower sound speeds (which result in a higher angle of intromission). Thus, when sound speed increases with depth, the angle of intromission increases with frequency up to a certain frequency above which it remains constant (associated with the sound speed at the water-sediment interface). In brief, the frequency dependence of the angle of intromission is highly sensitive to and thus contains information about the depth dependence of the mud sound speed profile.

The bottom loss data, Fig. 2(a), are therefore used to assess inferred mud sound speed profiles with large gradients.[2,3,5] Each of the sound speed profiles are used to predict bottom loss, assuming a constant density 1600 kg/m^3 and attenuation 0.3 dB/m/kHz over the upper 1.7 m. The assumed attenuation is inconsequential for the comparisons, inasmuch as it primarily affects the bottom loss at the angle of intromission, but not the angle of intromission itself (which is the quantity that is highly sensitive to the sound speed profile). We also make the assumption that the mud sound speed

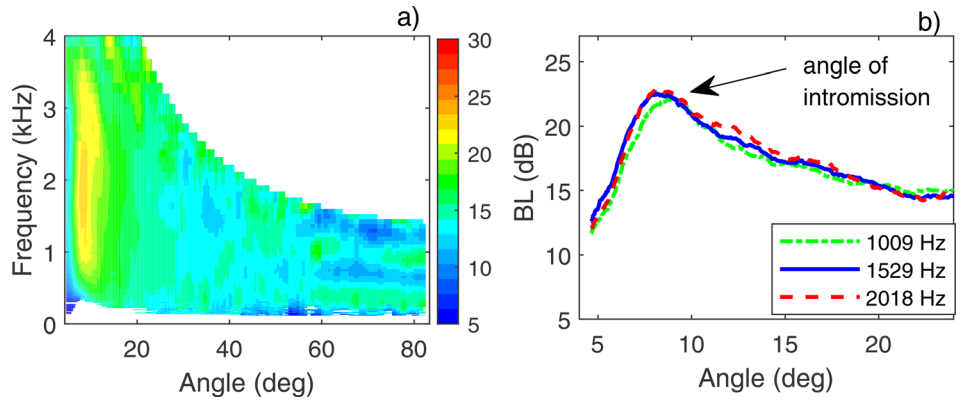

Fig. 2. Measured reflection data (bottom loss, in dB) in 1/15th octave bands at the SWAMI site, (a) across frequency (b) for selected frequencies where the angle of intromission is nearly frequency independent.

is constant over the frequency range of interest; see Refs. 5 and 7. The bottom loss is calculated from the spherical wave reflection coefficient, which is the exact solution for this geometry [see Eq. (2) in Ref. 14].

The frequency dependencies of the angle of intromission predicted by the sound speed profiles in Refs. 2 and 3 are shown in Figs. 3(a) and 3(b). Each result is compared with the measurements, Fig. 3(d), and discussed in the following.

Maximum entropy statistical analysis was applied to 25–275 Hz long-range propagation data[2] averaged in a 6.5 km radius around an array near the SWAMI site (blue triangle in Fig. 1). The analyses resulted in effective sound speed gradients of order 10 s−1 with a sound speed ratio at the water-mud interface of 0.977, see Fig. 3(c). Our bottom loss predictions, Fig. 3(a), from the mud sound speed profile in Ref. 2 show that below ∼1 kHz, the angle of intromission decreases due to the gradient. However, the measured data [Fig. 3(d)] show the opposite trend. This indicates that the sound speed gradient is too large. Secondarily and of less importance to the central topic here, the data show an angle of intromission of 8° above 1 kHz, whereas Ref. 2 predicts 12°, in other words, the sound speed ratio in Ref. 2 is somewhat too low.

A different long-range propagation data set, 20–100 Hz (cyan line in Fig. 1) and analysis technique[3] resulted in sound speed gradients of 20 s^{-1} with a sound speed ratio at the water-mud interface of 0.948; bottom loss predictions are shown in Fig. 3(b). At low frequencies, the high sound speed gradient leads to an even stronger increase in the angle of intromission with frequency; this is because the gradient is twice as large as that in Ref. 2. This behavior does not agree with the measured angle of intromission data. Also, note that above ∼500 Hz, the sound speed profile from Ref. 3 predicts an angle of intromission of ∼17°, more than twice that of the measured data, Fig. 3(d), in other words the sound speed ratio in Ref. 3 is far too low.

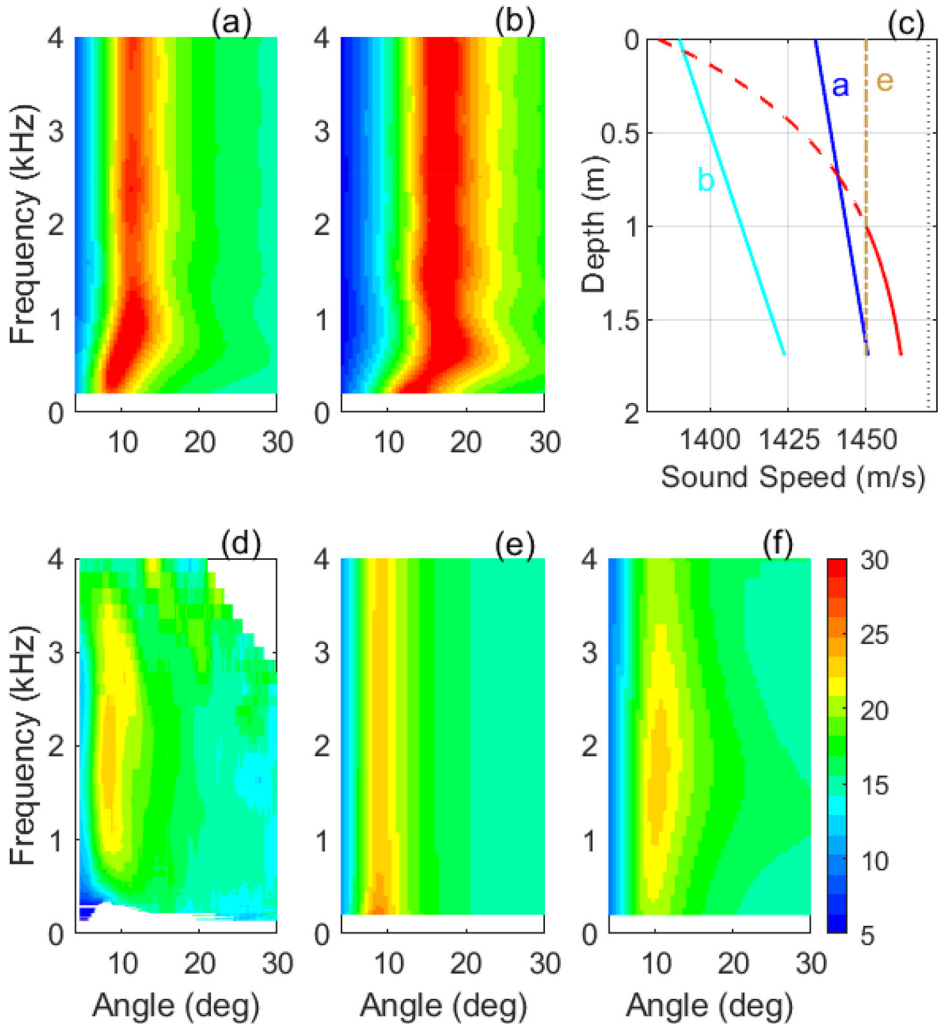

Fig. 3. Bottom loss measured data (d) and predictions from the upper 1.7 m of mud from various methods: (a) (Ref. 2), (b) (Ref. 3), (e) isospeed, and (f) single 0.53 m layer. Sound speed profiles for the various cases normalized to 1470 m/s (dotted black line) are given in (c) including the exponential profile from Ref. 5, where extrapolated values are shown as a dashed line. The profile from (f) is within a linewidth of profile (e). The basement sound speed for each profile is identical to the deepest value.

In both these long-range propagation analyses[2,3] the authors made an *a priori* assumption that the sound speed profile changes linearly with depth (i.e., a constant gradient) over the mud layer and note that this assumption may not be correct. It appears that the assumption is not correct; the disagreement in both cases with the bottom loss measurements indicates that the mud sound speed is not strongly increasing with depth over the upper few meters.

Could the disagreement be explained by sediment sound speed dispersion? It seems very unlikely. In Ref. 7, the dispersion was shown to be very small in the mud, less than 1 m/s per second over the measurement band, 400–1200 Hz, independent of depth in the upper 6 m of mud. Viscous Grain Shearing model[15] parameters were estimated from the same data,[7] which permits extrapolation in frequency of the sound speed; it shows less than 3 m/s dispersion between the lowest frequency of the propagation data, 20 Hz to 1200 Hz. Furthermore, *in situ* probe measurements showed a negligible dispersion in a higher band 2–10 kHz (Ref. 5) also independent of depth. Thus, there is strong evidence that the dispersion in this mud is very weak from 0.02–10 kHz over the upper few meters of sediment and that the high sound speed gradients, ∼10 m/s, cannot be explained by dispersion.

In situ probe measurements have an advantage of not requiring any assumptions or parameterization of the mud sound speed profile. Analyses of the sediment acoustic measurement system (SAMS) 2–10 kHz *in situ* probe data were averaged from 18 of the core locations between 1 and 3 m sub-bottom. The authors indicate that the measurements are best fit with an exponential[5] sound speed depth dependence, Fig. 3(c), where the continuation of the exponential profile above 1 m is shown by a dashed line. This continuation is unsupported by measurement. Bottom loss predictions with this profile are similar to Fig. 3(b), but with an even steeper decrease in the angle of intromission below 1 kHz, due to the higher gradient. The decrease in the angle of intromission below 1 kHz is controlled by the estimated gradient from the SAMS measurements from 1 to 1.7 m (solid line). However, this trend disagrees with the angle of intromission data, i.e., the sound speed gradient is too high.

Inspection of the reflection data yield clues as to the nature of the *in situ* sound speed profile. For a homogeneous half-space, the angle of intromission is independent of frequency. This is shown in Fig. 3(e), for a sound speed and density ratio 0.9865 and 1.557, respectively (the small increase in loss at the low frequency angle of intromission is due to spherical wave effects). The measured data, in fact do show more than an octave in which the angle of intromission, ∼8°, is nearly independent of frequency. This suggests that whatever sound speed deviations exist, they are small, especially when considered in relation to other sound speed profiles considered thus far.

Besides the near constancy of the angle of intromission over a broad frequency range, the data also indicate the presence of a Bragg interference pattern. Bragg's law gives the condition for constructive interference and for a sediment layer j, is $k_j d_j \sin(\theta_j) = n\pi$, where k is the wavenumber, d is layer thickness, θ is grazing angle, and n is an integer. The low-loss interference peak that cuts through near the angle of intromission at ∼4 kHz is from Bragg constructive interference. Solving for layer thickness, Braggs law indicates that the scale of the layer that caused it is ∼0.5 m. This is borne out by model predictions for a 0.53 m layer at the water-mud interface, which leads to bottom loss [Fig. 3(f)] reasonably similar to the observations. The mud sound speed and density in the 0.53 m layer is just 2 m/s and 40 kg/m^3 lower than the bottom half-space (which has sound speed and density ratios 0.9865 and 1.557, respectively). These geoacoustic properties are not intended to be presented as definitive values, but rather to demonstrate that depth-dependent sound speed changes in the upper few meters must be rather modest.

In summary, reflection data exhibiting an angle of intromission over a wide frequency range, 200–4000 Hz, contain significant information on mud sound speed depth-dependence. These data indicate that (1) large sound speed gradients of order 10 s^{-1} do not represent the *in situ* sound speed profiles and (2) the *in situ* sound speed and density of the mud are nearly constant over the upper 2 m at the SWAMI site.

3. Discussion

In this section, additional evidence is presented on the mud sound speed depth dependence in the upper 2 m of mud, as well as deeper in the mud layer. We draw upon additional long-range propagation measurements, the depth dependence of mud porosity in cores, and reflection coefficient data.

3.1 Inferences from other long-range propagation measurements

In Ref. 16, 10–80 Hz long-range propagation data in the thick mud region of NEMP show remarkably clear Airy phase structure and these data are used to invert for the sound speed ratio and the sound speed gradient, which is assumed to be constant (as in Refs. 2 and 3). When the Airy phase information is included a gradient of 9 s^{-1} is obtained, but the authors observe that there is an ambiguity between the sound speed ratio and the gradient. In a later paper,[17] the ambiguity was approximately removed, and the gradient was estimated to be 1.8 ± 1 s^{-1}.

The same assumption of a constant sound speed gradient in the mud layer is used in Ref. 4, where 50–250 Hz long-range propagation data in the NEMP thick mud region yield a sound speed gradient of ∼10 s^{-1}. In a later study,[9] the same authors removed the *a priori* assumption of a constant gradient and found that the sound speed in the upper 9 m of mud is constant, i.e., the sound speed gradient is 0 s^{-1}. Using higher signal-noise-ratio data with a larger

bandwidth, 10–400 Hz, the results indicated a constant mud sound speed over the upper 8 m, with a strong gradient below that to the top of the sand layer.

These studies show that when a constant mud sound speed gradient is assumed, large gradients result, and that ambiguities between the gradient and other parameters can exist. When the assumption of a constant mud sound speed gradient is removed, the mud sound speed is nearly constant with depth, at least in the upper 8–9 m at the NEMP thick mud region.

3.2 Porosity depth-dependence: Cores

A strong correlation exists between sediment sound speed and porosity. These correlations are evident, for example, in the empirical relations of Hamilton-Bachman.[18] As another example, the simple Mallock-Wood equation[19] has considerable explanatory power—for mud in particular—where sound speed depends primarily on the porosity (seawater and grain properties tend to be reasonably well-known). Thus, given that sound speed and porosity are tightly coupled, some insight into depth-dependent sound speed can be had from depth-dependent porosity measurements.

Extensive coring was undertaken in the NEMP area (see Fig. 1) including piston cores, gravity cores, vibracores, and acoustic cores.[15] Chaytor *et al.*[20] provide analysis from an extensive subset of those cores, identifying three lithostratigraphic units. The most pertinent is the uppermost geologic unit, unit 1, which is mud comprised predominantly of silt with smaller parts clay and sand. In the central part of the experiment area, where mud thickness exceeds 6 m, unit 1 extends at least to 3 m sub-bottom. The core data show a nearly depth-independent porosity over the upper 4 m and often deeper in the central region of the NEMP, see, e.g., Fig. 15 in Ref. 20. The depth-independent porosity indicates that the sound speed should also be constant, or nearly so, with depth. The remarkably consistent properties of the unit 1 mud extends not only in depth but in spatial extend across the SBCEX17 experiment area; the range of porosity values has a mean of 0.60 and standard deviation of only 0.04.[20] In summary, this uniformity strongly suggests that (a) sound speed in the upper 2 m is nearly constant, which independently supports the conclusions drawn from the angle of intromission observations and (b) that the nearly constant porosity extends much deeper than 2 m in the central region of the experiment area.

3.3 Sound speed and porosity depth-dependence: Reflection data

A Bayesian inversion method was applied to reflection coefficient data at the SWAMI site.[7] Those data are independent of the reflection data in Fig. 2, and used a time window large enough to include multiple sand horizons below the mud layer (10.3 m thick) to a depth of 16 m sub-bottom. Thus, there was a critical angle, but no angle of intromission. The results yielded a porosity nearly independent of depth over the upper 9 m, the sound speed is likewise nearly independent of depth over the upper 9 m, see Fig. 4. In the lower 1.3 m of the mud layer, the sound speed is observed to increase extremely rapidly from ∼1460 m/s to ∼1660 m/s. This is termed the sand-mud transition interval, which exhibits rapidly increasing sand content with depth. It is believed that the sand was entrained in the deposited mud by biologic mixing during the time period in which the first meter or so of mud was accumulating over top of the sand layer.

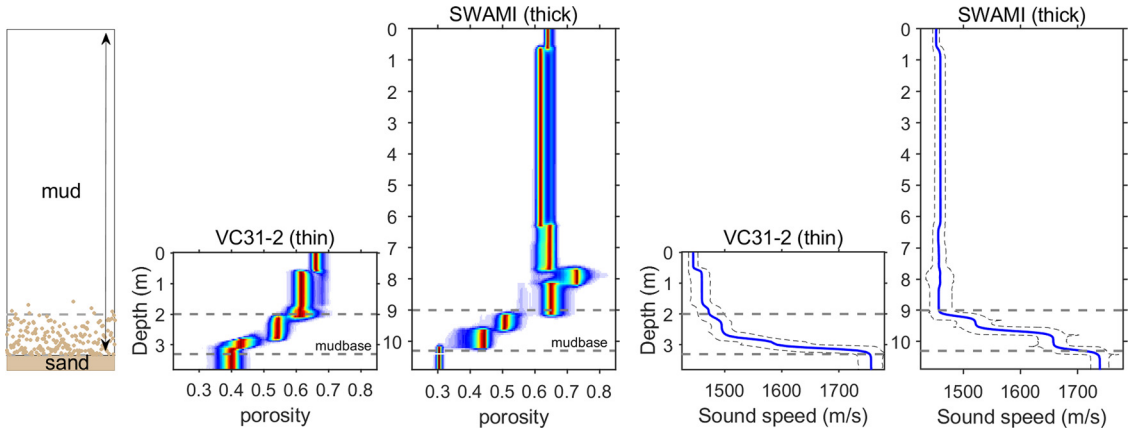

Fig. 4. Mud layer structure. From left to right: cartoon illustrating the sand-mud transition interval; porosity profiles at two sites (thin and thick mud layers) and sound speed profiles (450 Hz) at the same two sites. For the sound speed profiles, the thick lines indicate the mean and thin (dashed) lines indicate the 95% highest probability density credibility intervals from Bayesian inversion. The term "mud layer" is defined from the water-sediment interface (0 m) to the mudbase (lower dashed line). The sand-mud transition interval (between horizontal dashed lines) exhibits a decreasing porosity and increasing sound speed to the mudbase. Below the mudbase is sand. The plots are aligned at the mudbase to highlight the similarity of transition interval at two disparate sites. The bottom water sound speed is 1471/1474 m/s at the thin/thick mud site respectively (adapted from Ref. 21).

It useful to note that while the long-range propagation data inversions [Figs. 3(a) and 3(b)] imposed a constant gradient on a ∼10 m thick mud layer, the Bayesian inversion[7] employed a trans-dimensional framework in which the data determined the number of layers and the properties of each layer were arbitrary; that is to say that no assumptions were imposed on the form of the depth dependence. The trans-dimensional results[7,9] are in agreement with (but were not informed by) the core data in the overall depth dependence of both the porosity and the sound speed. Thus, it appears that the large mud layer sound speed gradients from the long-range propagation inversions were caused by the constant gradient assumption on the entire mud layer, where the evidence points to strong gradients only in the lower (1.3 m) transition interval.

Although the mud layer, for geologic reasons, was defined to include both homogeneous mud and mud with large amounts of sand (the transition interval), it is helpful from a sediment acoustics point of view to separate these two kinds of disparate sediments. Thus, the evidence from both the angle of intromission data and the trans-dimensional results indicates that in the relatively homogeneous part of the mud layer (the upper 9 m at SWAMI site), the sound speed was nearly independent of depth. That is to say that in the NEMP mud (ignoring the transition interval), the sound speed gradient is very small or zero.

How do these conclusions depend on location within the SBCEX17 experiment area? Figure 4 also shows results from reflection coefficient analysis at a site ∼15 WNW of SWAMI where the mud is quite thin. The salient result is that the mud above the transition interval, also exhibits a relatively uniform porosity and sound speed. Note that a both sites there is a ∼0.5 m thick surficial layer with a slight increase in porosity and slight decrease in sound speed and this may accord with the observed Bragg line in the angle of intromission data presented here. The main point, however, is that the reflection data results at these two widely separated sites, with markedly different sediment thickness, show (as do the unit 1 core data), that the mud properties above the transition interval are fairly uniform in geographic location and in depth.

4. Conclusions

The mud at the New England Mud Patch exhibits a nearly uniform sound speed in the upper few meters and likely down to a meter or so above the sand layer. The evidence from the upper few meters comes from broadband angle of intromission data, confirmed by independent core and other reflection coefficient data. The latter two data sources provide evidence for the relative sound speed uniformity in nearly the entire mud layer. It would be inappropriate to infer that all shallow-water muds exhibit similar behavior. The NEMP mud is predominantly silt and thus the depth dependence of sound speed may vary for other mud mixtures. In summary, strong evidence indicates that sound speed gradients in the NEMP mud above the sand-mud transition layer are small, much less than the order $10\,s^{-1}$ gradients that have been suggested.

Acknowledgments

The author gratefully acknowledges the financial support of the ONR Ocean Acoustics program, the captain and crew of the R/V Armstrong for their considerable skill and energy, Preston Wilson and David Knobles as Chief Scientists for SBCEX17, and Stan Dosso, Jie Yang, and Darrell Jackson for helpful comments on the manuscript.

References and links

[1]P. S. Wilson, D. P. Knobles, and T. A. Nielsen, "Guest editorial: An overview of the Seabed Characterization Experiment," IEEE J. Ocean Eng. **45**, 1–13 (2020).
[2]D. P. Knobles, P. S. Wilson, J. A. Goff, L. Wan, M. J. Buckingham, J. D. Chaytor, and M. Badiey, "Maximum entropy derived statistics of sound-speed structure in a fine-grained sediment inferred from sparse broadband acoustic measurements on the New England continental shelf," IEEE J. Ocean Eng. **45**, 161–173 (2020).
[3]Y.-T. Lin, J. Bonnel, D. P. Knobles, and P. S. Wilson, "Broadband waveform geoacoustic inversions with absolute travel time," IEEE J. Ocean Eng. **45**, 174–188 (2020).
[4]J. Bonnel, Y.-T. Lin, D. Eleftherakis, J. A. Goff, S. E. Dosso, R. Chapman, J. H. Miller, and G. R. Potty, "Geoacoustic inversion on the New England Mud Patch using warping and dispersion curves of high-order modes," J. Acoust. Soc. Am. **143**, EL405–EL411 (2018).
[5]J. Yang and D. R. Jackson, "Measurement of sound speed in fine-grained sediments during the seabed characterization experiment," IEEE J. Ocean Eng. **45**, 39–50 (2020).
[6]E. L. Hamilton, "Geoacoustic modeling of the seafloor," J. Acoust. Soc. Am. **68**, 1313–1340 (1980).
[7]J. Belcourt, C. W. Holland, S. E. Dosso, and J. Dettmer, "Depth-dependent geoacoustic estimates with dispersion from the New England Mud Patch via reflection coefficient inversion," IEEE J. Oceanic Eng. **45**, 69–91 (2020).
[8]D. Tollefsen and S. E. Dosso, "Ship source level estimation and uncertainty quantification in shallow water via Bayesian marginalization," J. Acoust. Soc. Am. **147**, EL339–EL344 (2020).
[9]J. Bonnel, S. E. Dosso, D. Eleftherakis, and N. R. Chapman, "Trans-dimensional inversion of modal dispersion data on the New England Mud Patch," IEEE J. Ocean. Eng. **45**, 116–130 (2020).
[10]M. S. Ballard, K. M. Lee, A. R. McNeese, P. S. Wilson, J. D. Chaytor, J. A. Goff, and A. H. Reed, "*In Situ* measurements of compressional wave speed during gravity coring operations in the New England Mud Patch," IEEE J. Ocean Eng. **45**, 26–38 (2020).
[11]C. W. Holland, J. Dettmer, and S. E. Dosso, "Remote sensing of sediment density and velocity gradients in the transition layer," J. Acoust. Soc. **118**, 163–177 (2005).

[12]G. R. Venegas, J. D. Sagers, and P. S. Wilson, "Laboratory measurements and simulations of reflections from a water/clay interface during the diffusion of salt," J. Acoust. Soc. Am. **146**(2), 1384–1393 (2019).
[13]C. W. Holland, C. Smith, Z. Lowe, and J. Dorminy, "Seabed observations at the New England Mud Patch: Reflection and scattering measurements and direct geoacoustic information," IEEE J. Ocean Eng. (in press).
[14]C. W. Holland, P. L. Nielsen, J. Dettmer, and S. E. Dosso, "Resolving meso-scale seabed variability using reflection measurements from an autonomous underwater vehicle," J. Acoust. Soc. Am. **131**, 1066–1078 (2012).
[15]M. J. Buckingham, "On pore-fluid viscosity and the wave properties of saturated granular materials including marine sediments," J. Acoust. Soc. Am. **122**, 1486–1501 (2007).
[16]L. Wan, M. Badiey, D. P. Knobles, and P. S. Wilson, "The Airy phase of explosive sounds in shallow water," J. Acoust. Soc. Am. **143**(3), EL199–EL205 (2018).
[17]L. Wan, M. Badiey, D. P. Knobles, P. S. Wilson, and J. Goff, "Estimates of low-frequency sound speed and attenuation in a surface mud layer using low-order modes," IEEE J. Ocean Eng. **45**, 201–211 (2020).
[18]R. T. Bachman, "Acoustic and physical property relationships in marine sediment," J. Acoust. Soc. Am. **78**, 616–621 (1985).
[19]A. B. Wood, *A Textbook of Sound* (G. Bell, London, UK, 1964).
[20]J. D. Chaytor, M. S. Ballard, B. J. Buczkowski, J. Z. Goff, K. M. Lee, A. H. Reed, and A. A. Boggess, "Measurements of geologic characteristics and geophysical properties of sediments from the New England Mud Patch," IEEE J. Ocean Eng. (in press).
[21]C. W. Holland and S. E. Dosso, "On compressional wave attenuation in muddy marine sediments," J. Acoust. Soc. Am. **149**, 3674 (2021).